

# *Broadband Dielectric Spectroscopy and Scattering Techniques*

*Alexei Sokolov*

*UT/ORNL Joint Institute for Neutron Sciences*

## **Helpful Literature for Neutron Scattering:**

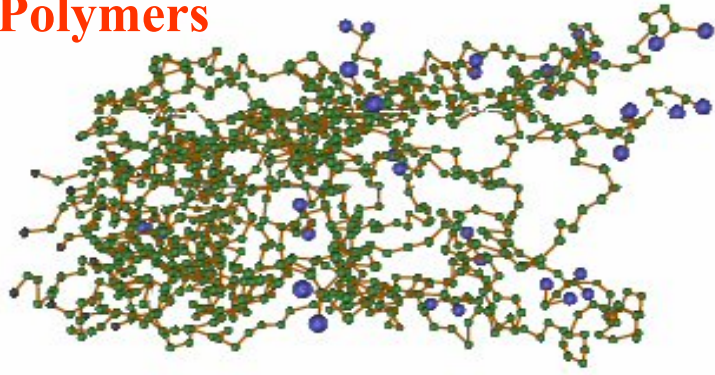
- **Dynamics of Soft Matter: Neutron Applications**, Eds. V. Garcia Sakai, C. Alba-Simionesco, S.H. Chen (Springer, 2011)
- **Polymers and Neutron Scattering**, J.Higgins, H.Benoit
- Richter, et al., **Adv.Pol. Sci.** **174**, 1 (2005)



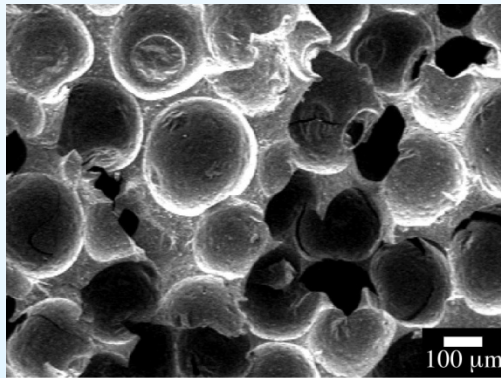
# Soft Matter

Wisla 2015

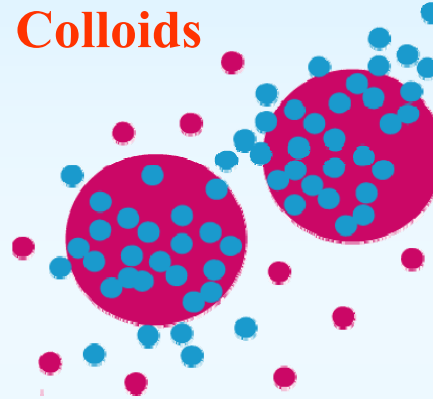
## Polymers



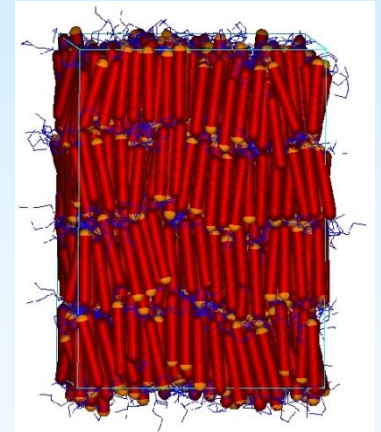
## Foams and Gels



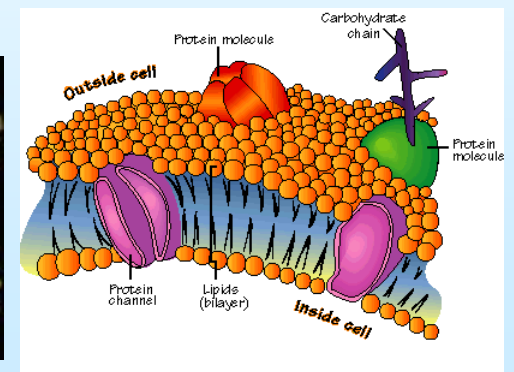
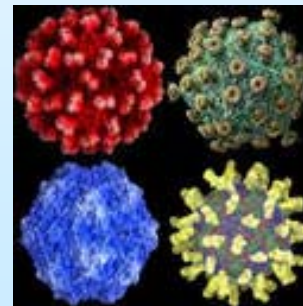
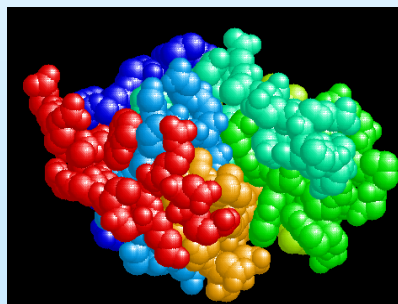
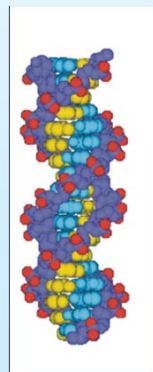
## Glass-forming Systems



## Liquid Crystals



## Biological Systems



---

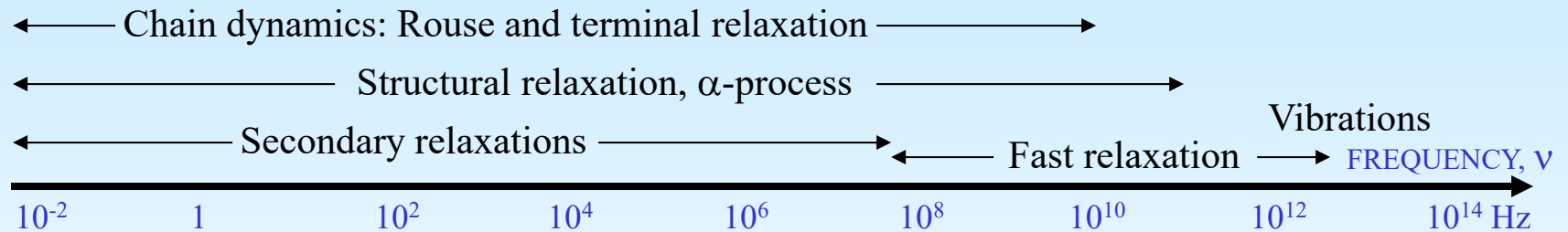
## Characteristics of Soft Materials:

- Variety of states and large number of degrees of freedom, metastable states
- Delicate balance between Entropic and Enthalpic contributions to the Free Energy
- Large thermal fluctuations and high sensitivity to external conditions
- Macroscopic softness

*Dynamics is the key to many macroscopic properties of Soft Materials*

# Frequency map of polymer dynamics

Wisla 2015



Mechanical relaxation  $G^*(\nu)$

Dielectric Spectroscopy,  $\epsilon^*(\nu)$

Quasi-optics, TDS

Traditional dielectric spectroscopy

IR-spectr.

Light Scattering,  $I_{ij}(Q, \nu)$

Interferometry

Photon – Correlation Spectroscopy

Raman spectroscopy

Spin-Echo

Neutron Scattering,  $S(Q, \nu)$

Back-sc.

Time-of-Flight

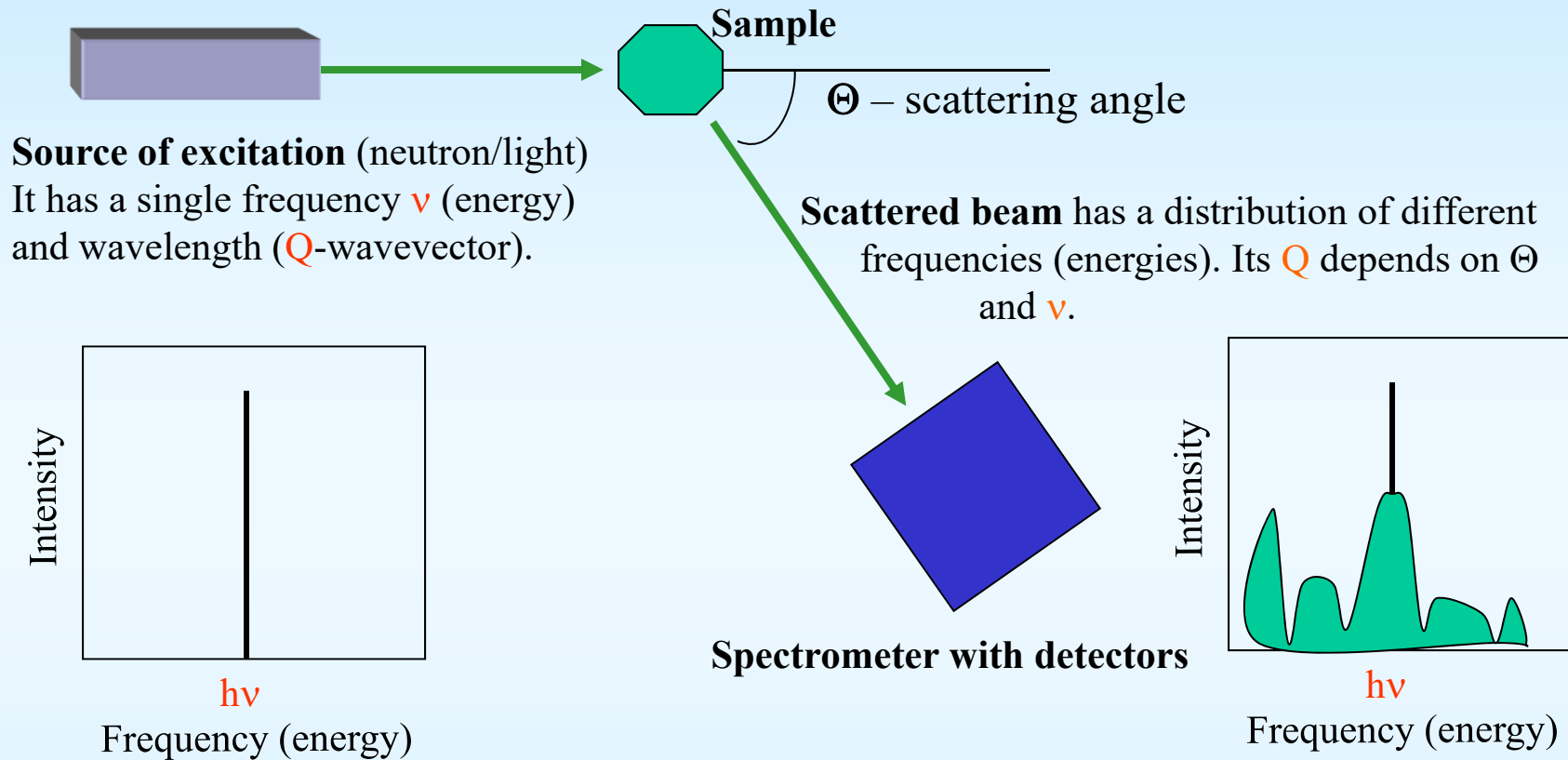
Inelastic X-ray Scattering,  $S(Q, \nu)$

High-Resolution  
IXS

Scattering techniques have an advantage due to additional variable – wave-vector  $Q$

# Scattering Techniques

Wisla 2015



Changes in the excitation frequency (energy) and wavevector are measured.

Changes in  $\nu$  brings information on characteristic frequencies or relaxation time  $\tau$  of molecular motions, while changes in  $Q$  brings information on direction and distances of the motions.

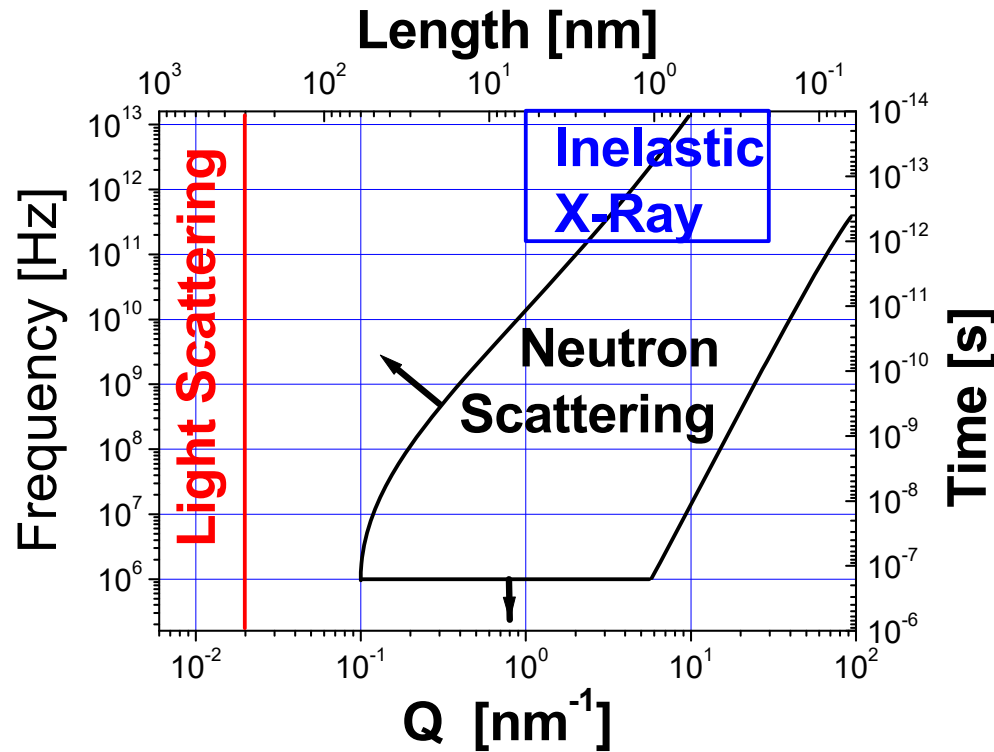


Table 3.1 Scattering lengths and cross section for some common isotopes

	$b \times 10^{12}$ (cm)	$\sigma_{\text{coh}} \times 10^{24}$ (cm <sup>2</sup> )	$\sigma_{\text{inc}} \times 10^{24}$ (cm <sup>2</sup> )	$\sigma_{\text{abs}} \times 10^{24}$ (cm <sup>2</sup> at 1.798 Å)
<sup>1</sup> H	-0.374	1.76	79.7	0.33
<sup>2</sup> D	0.667	5.59	2	0.0005
<sup>12</sup> C	0.665	5.55	0	0.003
<sup>14</sup> N	0.94	11.01	0.5	1.9
<sup>16</sup> O	0.58	4.23	0	0.0001
<sup>19</sup> F	0.57	4.02	0	0.0096
ave <sup>28.06</sup> Si	0.415	2.16	0	0.17
<sup>32</sup> S	0.28	1.02	0	0.53
ave <sup>35.5</sup> Cl	0.96	11.53	5.3	33.5

- Measures characteristic times (frequency) and geometry of the motions.
- Covers broad frequency and Q-range in the most important for microscopic dynamics region.
- Most of the soft materials contain hydrogen atoms, use of D/H contrast.
- Direct comparison to results of MD-simulations.

# What is Measured: *Time-Space Correlation Function*

Wisla 2015

In an isotropic medium, time-space pair correlation function:  $G(r,t) = \langle n(0,0)n(r,t) \rangle$

where  $n(r,t) = \sum_j^N \delta(r - r_j(t))$  presents coordinate of all atoms at time t.

$G(r,t)$  has self and distinct part,  $G(r,t) = G_s(r,t) + G_d(r,t)$ . If at time  $t_1=0$  a particle was at position  $r_1=0$ ,  $G_s(r,t)$  gives a probability to find the same particle around position  $r$  at time  $t$ , and  $G_d(r,t)$  gives a probability to find another particle around position  $r$  at time  $t$ .

Intermediate scattering function is a space-Fourier transform of  $G(r,t)$ :  $I(q,t) = \int_V G(r,t) \exp(iqr) d^3r$

Definition from quantum mechanics:  $I(q,t) = \sum_i \sum_j \langle \exp[-iqr_i(0)] \exp[+iqr_j(t)] \rangle = \sum_i \sum_j \langle \exp[-iq\{r_i(0) - r_j(t)\}] \rangle$

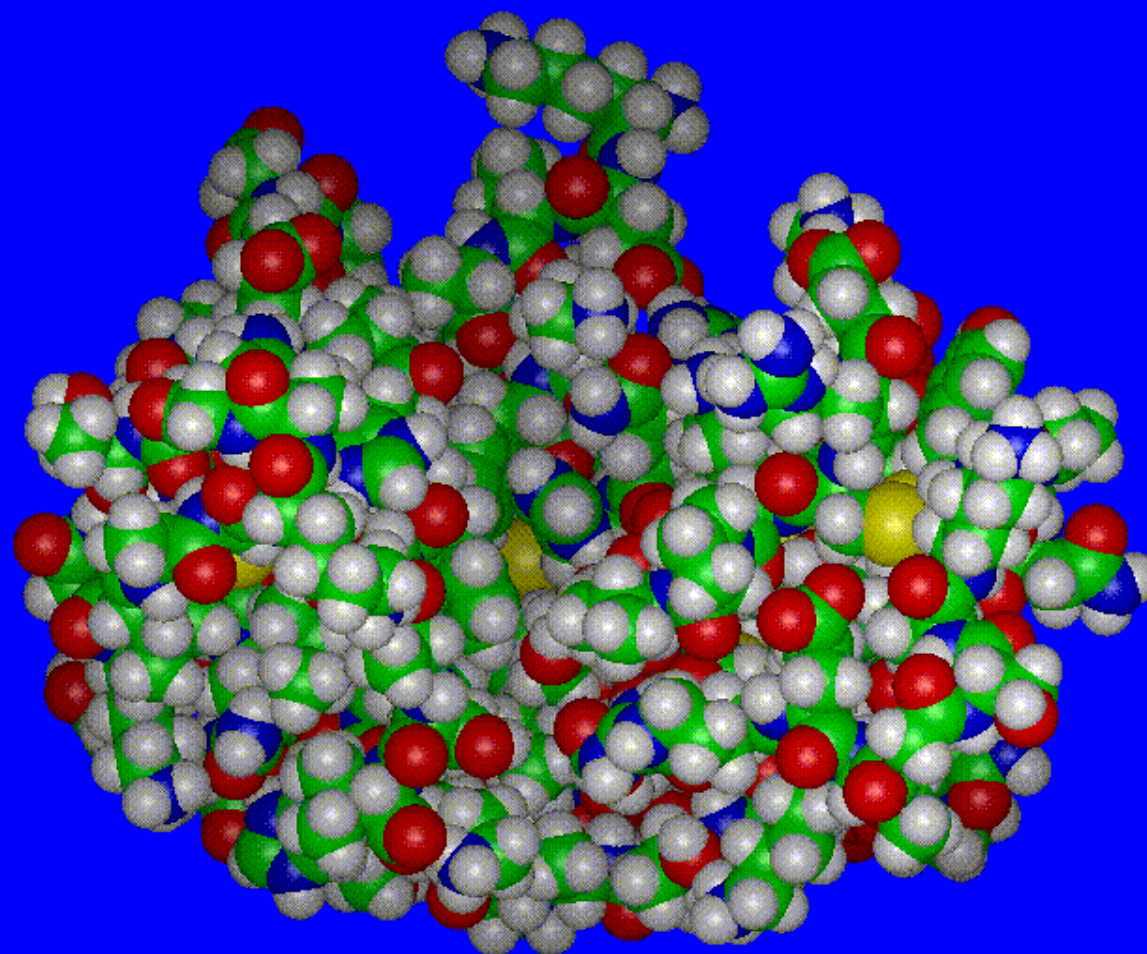
Time-Fourier transform of  $I(q,t)$  gives dynamic structure factor:  $S(q,\omega) = \frac{1}{2\pi} \int_{-\infty}^{\infty} \exp(-i\omega t) I(q,t) dt$

There are coherent and incoherent  $S(q,\omega)$ :  $S_{inc}(q,\omega) = \frac{1}{2\pi} \int_{-\infty}^{\infty} dt \int_V G_s(r,t) \exp[i(qr - \omega t)] d^3r$

$$S_{coh}(q,\omega) = \frac{1}{2\pi} \int_{-\infty}^{\infty} dt \int_V G_d(r,t) \exp[i(qr - \omega t)] d^3r$$

These equations were first introduced by van Hove [van Hove, *Phys.Rev.* **95**, 249 (1954)].

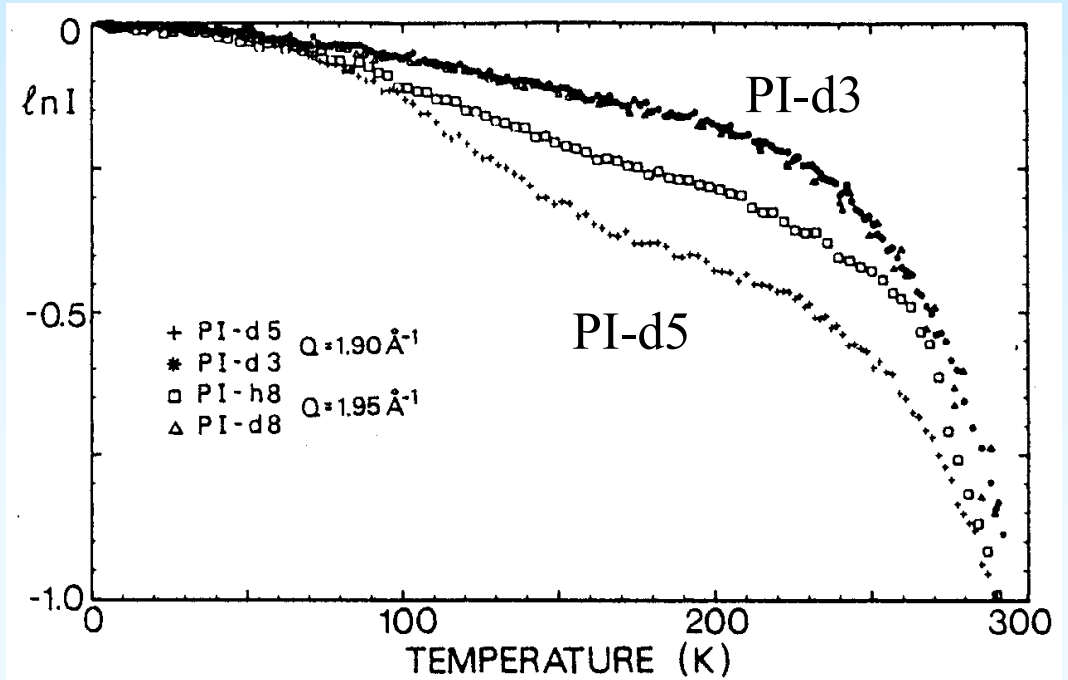
*Computer simulations of Ribonuclease A, 100 ps trajectory, Dr. M.Tarek, NIST*



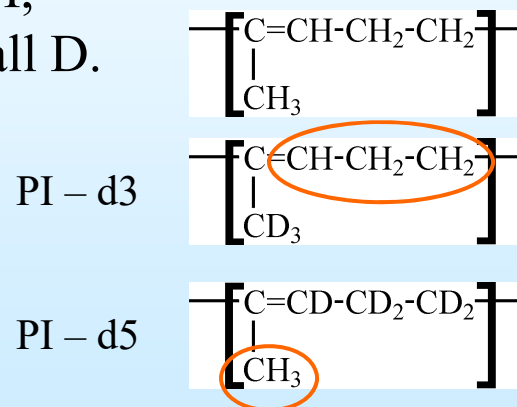
## Using H/D Contrast

An example of elastic scan measurements of PI [Frick, Fetters, *Macromol.* 27, 1994]. Decrease of elastic intensity marks onset of a relaxation process. Various deuteration of the polymer allows separate methyl group and main-chain motion.

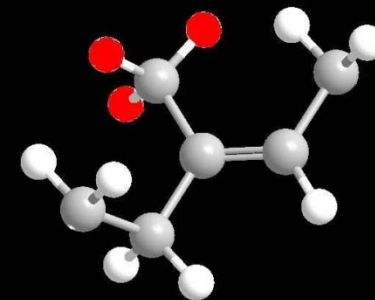
The onset of methyl groups rotation at temperatures below  $T_g$  is clearly seen.



PI-h8 – all H,  
PI-d8 with all D.



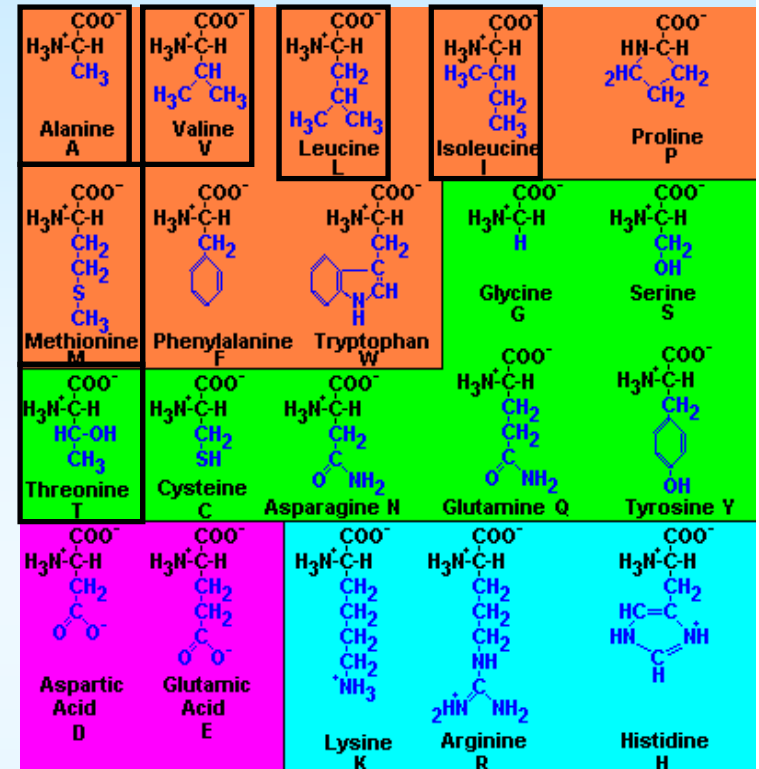
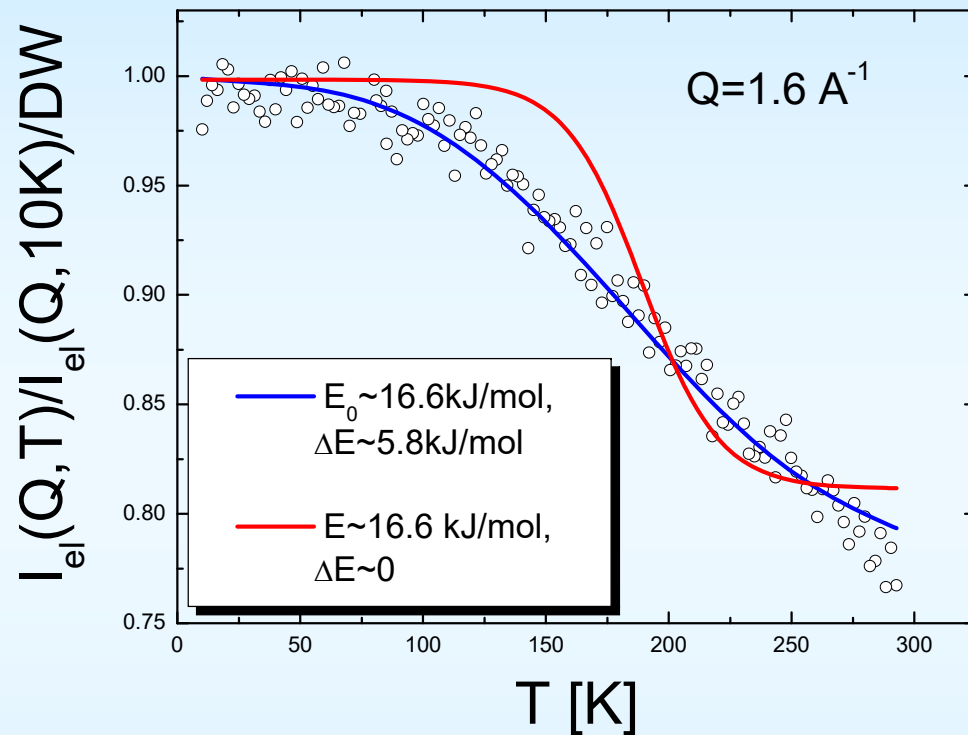
PI-d5



# Methyl Group Dynamics in Proteins

Wisla 2015

Significant part of H-atoms in proteins are on methyl groups.



Decrease of the elastic intensity in dry lysozyme can be described assuming a Gaussian distribution of energy barriers,  $g(E_i) \propto \exp[-(E_i - E_0)^2 / 2\Delta E^2]$ , with  $E_0 \sim 16.6 \text{ kJ/mol}$  and  $\Delta E \sim 5.8 \text{ kJ/mol}$  in good agreement with earlier NMR data [J.H.Roh, et al. *Biophys.J.* 91, 2573 (2006)].

$$I_{el}(Q, T, \omega \sim 0) = DW(Q, T) \left[ 1 - p_m + p_m \int_{-\infty}^{\infty} S_{met}(Q, \omega') R(\omega - \omega') d\omega' \Big|_{\omega=0} \right] \propto DW(Q, T) \left[ const(Q) + \int_{-\infty}^{\infty} R(\omega - \omega') \int_0^{\infty} g(E_i) \frac{\tau_i}{1 + \omega^2 \tau_i^2} dE_i d\omega' \Big|_{\omega=0} \right]$$

Here  $\tau_i = \tau_0 \exp(E_i / kT)$

# Estimates of the Mean-Squared Atomic Displacements

Wisla 2015

In first approximation (Gaussian), the elastic intensity  $I(Q,T)$ :

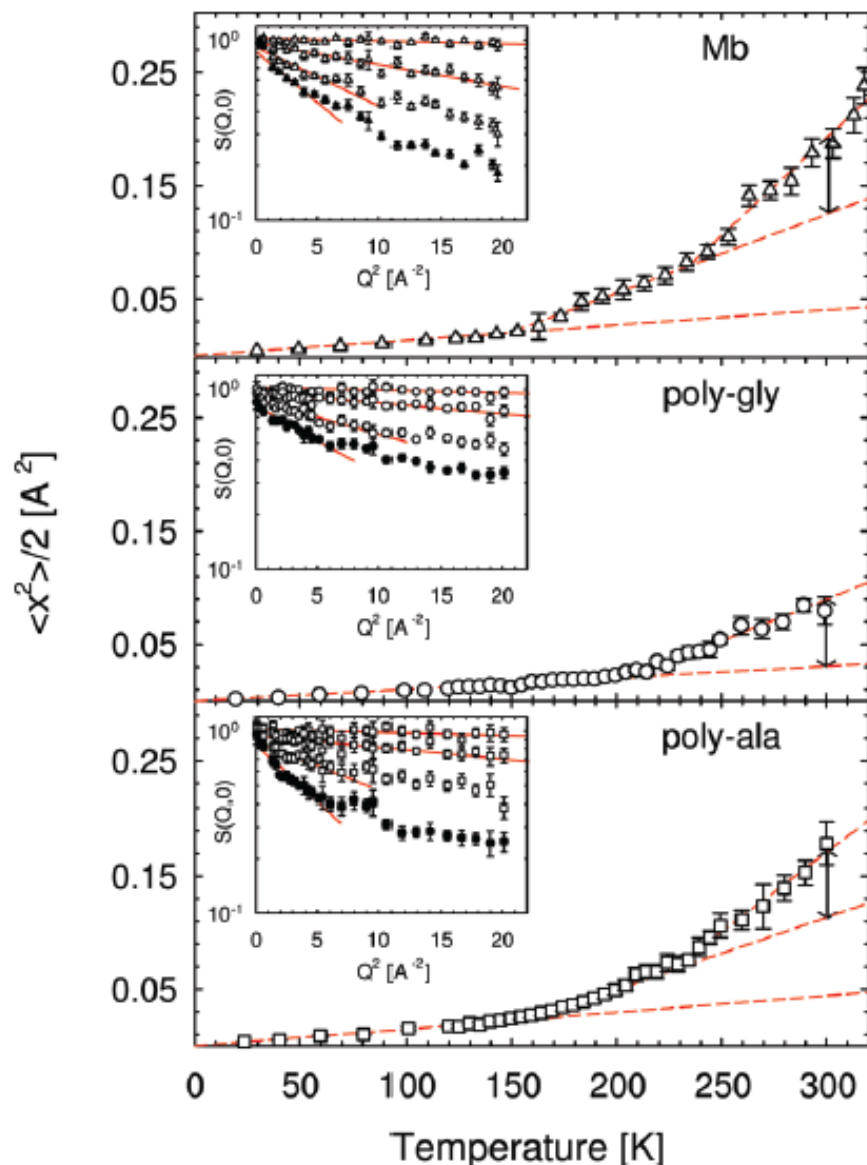
$$I(Q,T) \approx \exp\left(-Q^2 \frac{\langle x^2(T) \rangle}{2}\right)$$

Here  $\langle x^2 \rangle$  is the mean-squared displacement (MSD) along the scattering vector  $Q$  on the time scale defined by the spectrometer resolution. The total MSD for isotropic motions is  $\langle r^2 \rangle = 3\langle x^2 \rangle$

Usually MSD is estimated from the slope of  $\ln[I(Q,T)]$  vs  $Q^2$ . In most cases the initial  $I(Q)$  is estimated as the intensity measured at the lowest  $T$  (e.g.  $T=10K$ ), although normalization to Vanadium is more accurate.

Traditional approach:

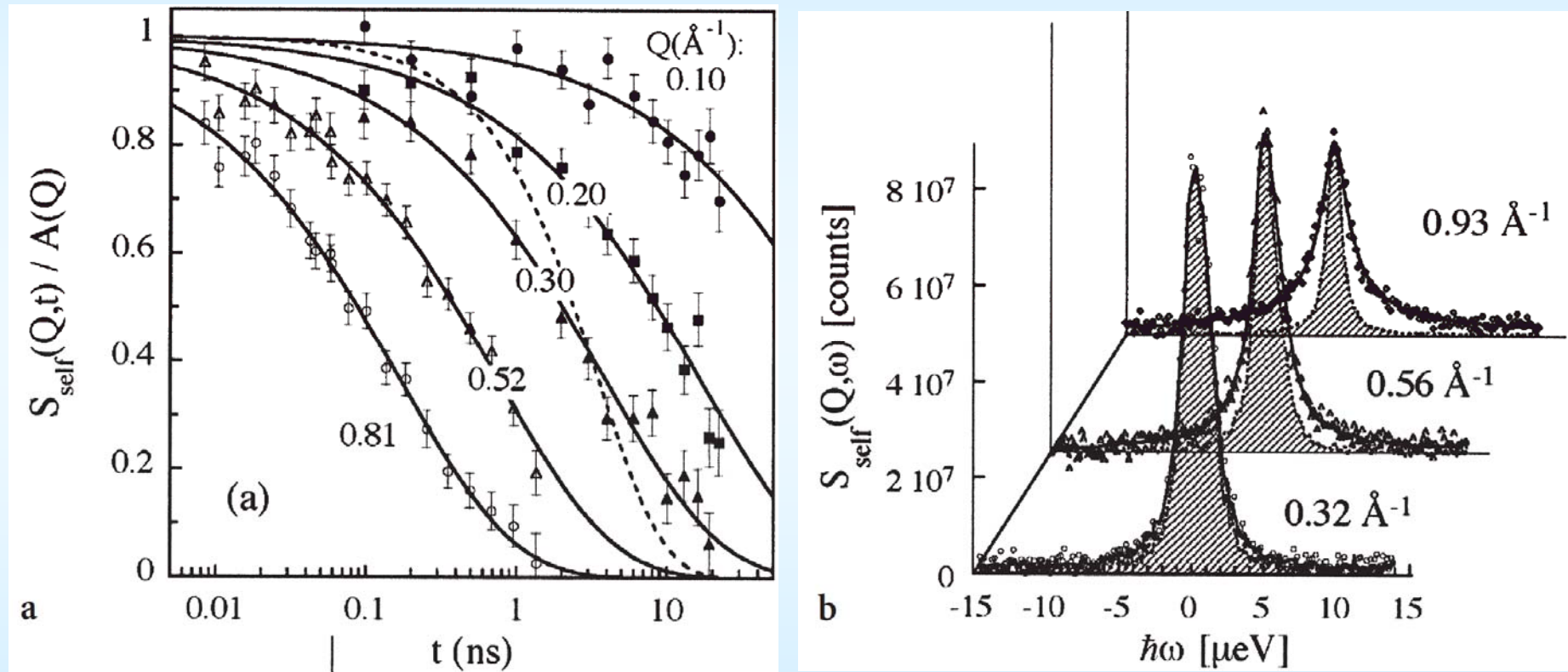
$$\langle r^2 \rangle \approx -\frac{6}{Q^2} \ln\left[\frac{I(Q,T)}{I(Q,T=10K)}\right]$$



# Analysis of Energy- or Time-Resolved Spectra

Wisla 2015

MSD is an integrated quantity. It includes diffusion, rotation and other local conformational motions and vibrations. Significantly more information can be gained from time- or energy- resolved spectra.



Intermediate scattering function  $S(Q,t)$  (a) and the dynamic structure factor  $S(Q,\omega)$  of PI-d3 measured at different  $Q$  and at  $T=340\text{K}$  [Richter, et al., *Adv.Pol. Sci.* 174, 1 (2005)].

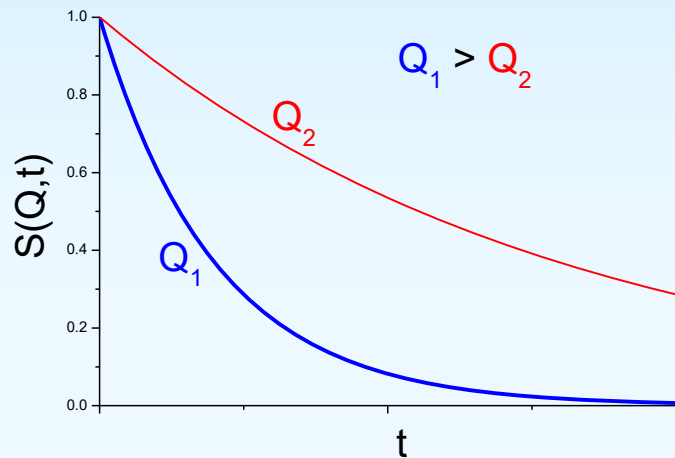
# Q-dependence: Diffusion

Wisla 2015

For regular diffusion:  $\langle r(t)^2 \rangle \propto Dt$

In that case:

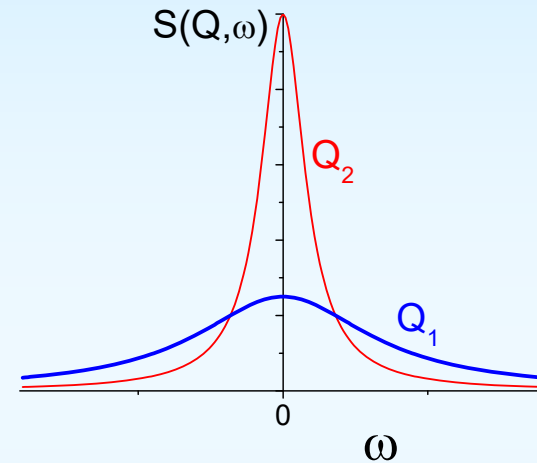
$$S_{inc}(Q, t) \propto \exp(-Q^2 Dt) = \exp(-\Gamma t)$$



An exponential decay for  $S(Q, t)$ , with decay rate  $\Gamma \propto Q^2$

In frequency domain:

$$S_{inc}(\omega, t) \propto \int \exp(i\omega t) \exp(-\Gamma|t|) dt = \frac{2\Gamma}{\Gamma^2 + \omega^2}$$



In the case of sub-diffusive regime:  $\langle r(t)^2 \rangle \propto (Dt)^\beta \Rightarrow S(Q, t) \propto \exp[-Q^2 (Dt)^\beta] \propto \exp[-(\Gamma t)^\beta]$   
with  $\Gamma \propto Q^{2/\beta}$ .

Diffusion-like motions exhibit strong dependence of the decay rate  $\Gamma$  (or relaxation time  $\tau \propto 1/\Gamma$ ) on  $Q$ .

# Q-dependence: Local Relaxation Process

Wisla 2015

Let's assume that there are two equal positions and molecule makes jumps between  $r_1$  and  $r_2$  positions. In isotropic case:

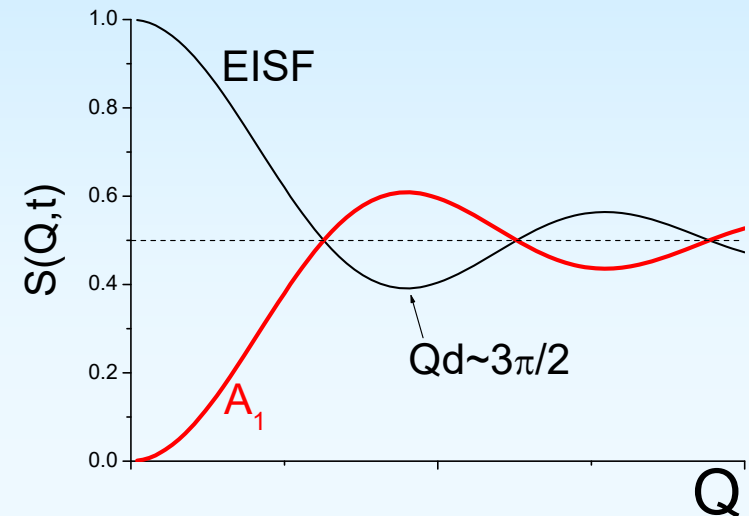
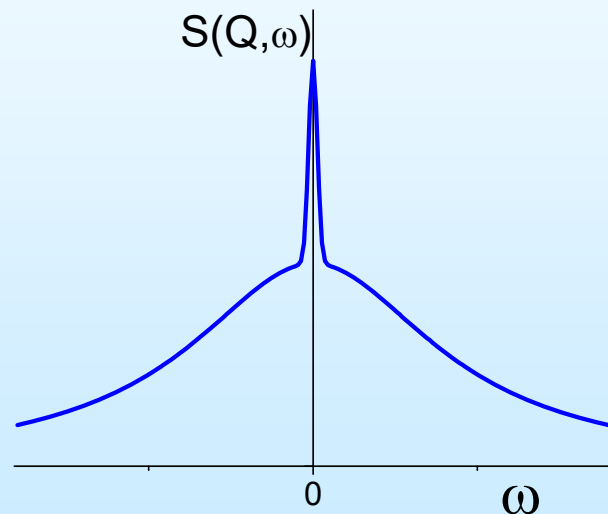
$$S_{inc}(Q, t) \propto [EISF(Q) + A_1(Q) \exp(-2t/\tau)]; d = r_2 - r_1$$

$$EISF(Q) = (1/2) \left\{ 1 + \frac{\sin Qd}{Qd} \right\}; A_1(Q) = (1/2) \left\{ 1 - \frac{\sin Qd}{Qd} \right\}$$

EISF(Q) is the Elastic Incoherent Structure Factor. It contains information on geometry of the motion.

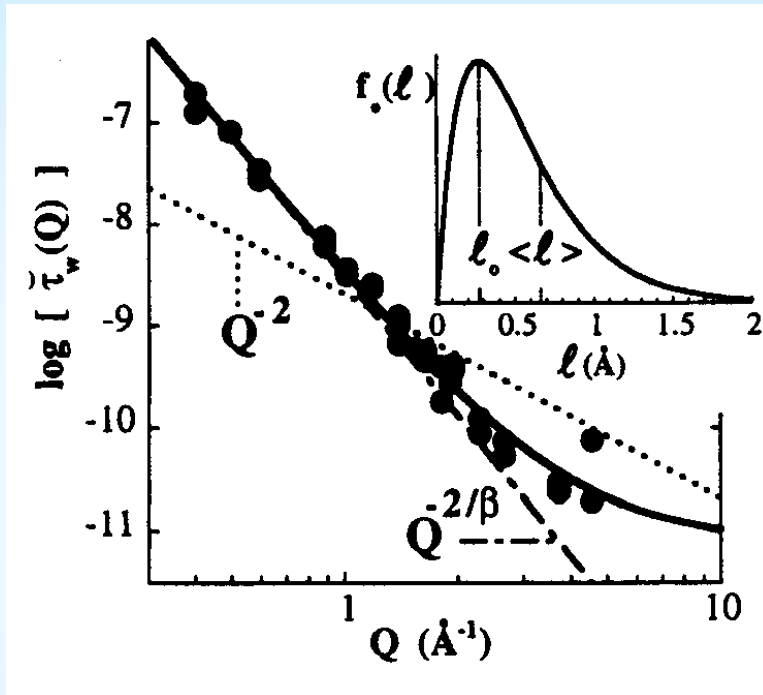
In the frequency domain:

$$S_{inc}(Q, \omega) = N \left[ EISF(Q) \delta(\omega) + A_1(Q) \frac{1}{\pi} \frac{2\tau}{4 + \omega^2 \tau^2} \right]$$



For a local relaxation process:

- ✓  $S(Q, \omega)$  has two component – elastic and quasielastic;
- ✓ Characteristic time scale  $\tau$  (or  $\Gamma$ ) is independent of  $Q$  (at least, at large  $Q$ ).



Segmental relaxation time  $\tau_s$  exhibits strong  $Q$ -dependence,  $\tau_s \propto Q^{-2/\beta}$ , indicating “stretched” diffusive-like process ( $\beta$  - KWW stretching parameter).

## Homogeneous vs Heterogeneous Dynamics

a) **Heterogeneous**: Normal diffusion with distribution of diffusion coefficient  $D$ :

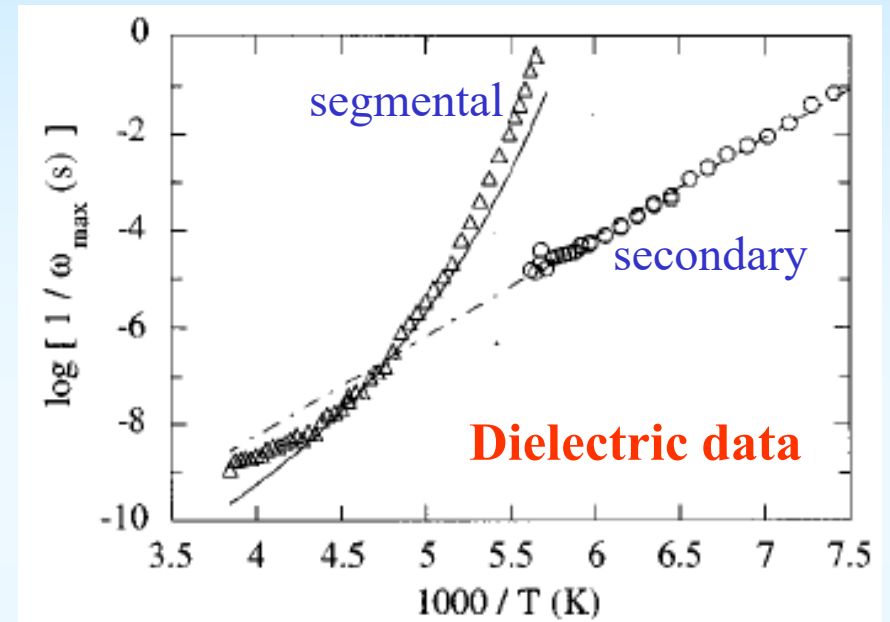
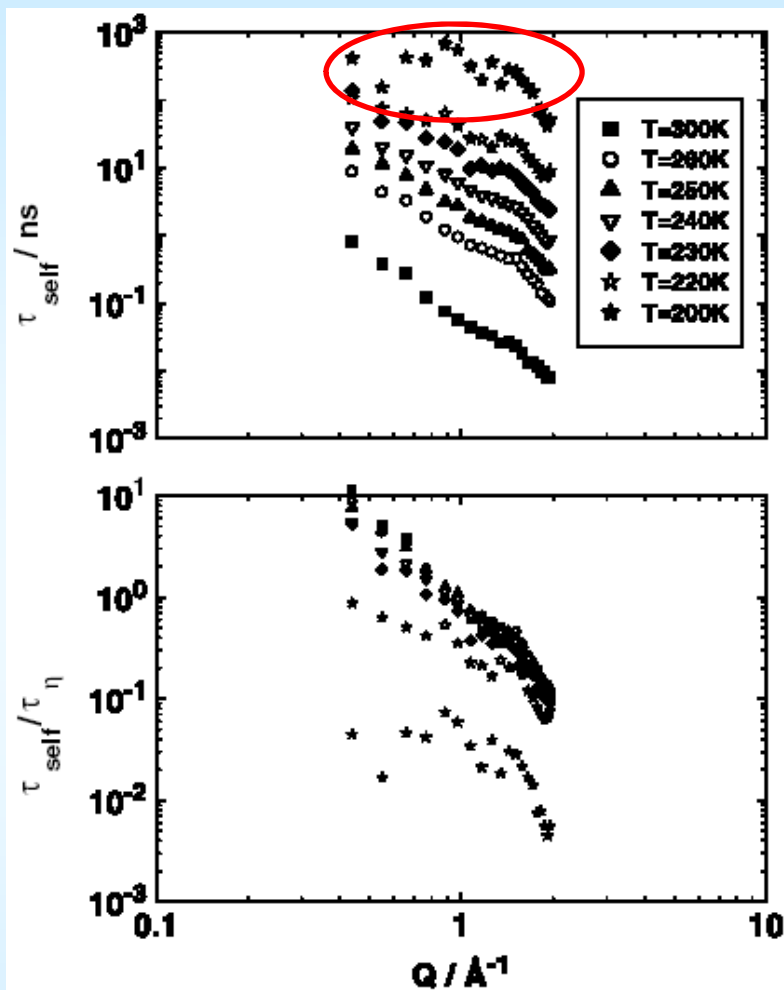
$$S(Q, t) = \int_{-\infty}^{\infty} g(\ln D^{-1}) \exp(-Q^2 D t) d(\ln D^{-1}) \propto \exp[-(Q^2 D t)^\beta]$$

$\tau \propto Q^{-2}$

b) **Homogeneous**: Sublinear diffusion in time,  $\langle r^2(t) \rangle \propto t^\beta$ :

$$S(Q, t) = \exp(-Q^2 \langle r^2(t) \rangle / 6) \propto \exp[-Q^2 (D t)^\beta]$$

$\tau \propto Q^{-2/\beta}$

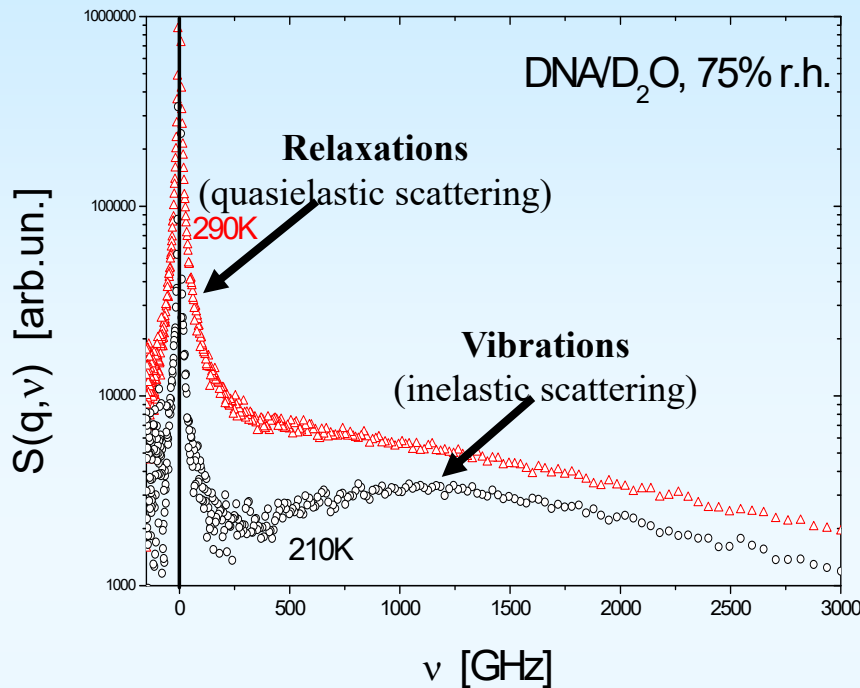


This behavior is ascribed to the split of segmental and secondary (local) relaxations.

$Q$  dependence of  $\tau_{\text{self}}$  change sharply when  $T$  approaches  $\sim 200\text{K}$ . Also scaling with the viscosity time scale  $\tau_{\eta}$  fails.

# Analysis of Quasielastic Spectra: $S(Q,E)$ vs $\chi''(Q,E)$

Wisla 2015

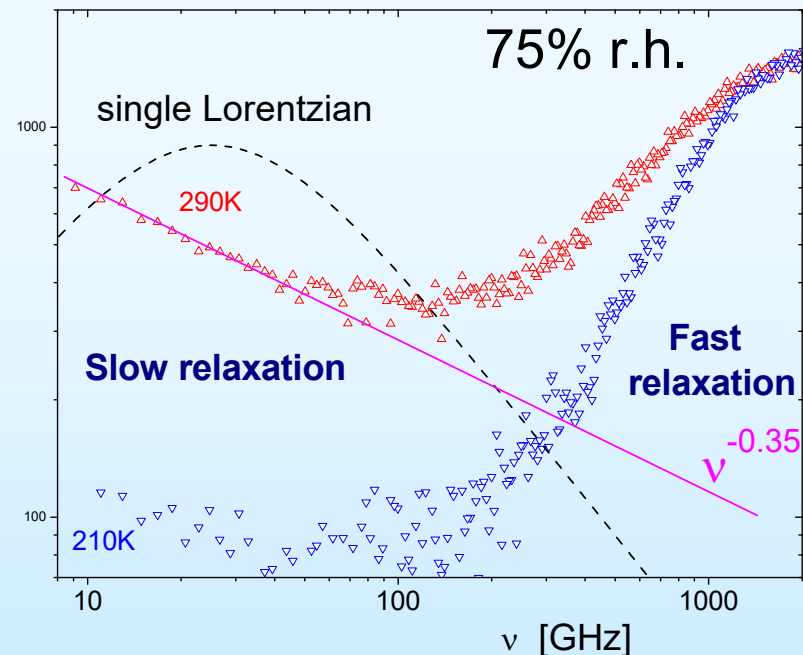


The quasielastic scattering (a relaxation-like contribution) usually dominates the spectra at higher T. It is traditionally approximated by a sum of a few Lorentzians. This approximation assumes a few single exponential relaxation processes. This assumption, however, can lead to misleading results.

Susceptibility presentation of relaxation spectra (here  $n(\nu)=[\exp(h\nu/kT)-1]^{-1}$  is the Bose factor) is very useful and has a few advantages:

- can be compared to  $\epsilon''(\nu)$ ,  $G''(\nu)$ ;
- each relaxation process appears as a maximum at  $2\pi\nu\tau\sim 1$ ;
- slopes of the tails give estimate of stretching exponents.

$$\chi''(q,\nu)=S(q,\nu)/n(\nu)$$

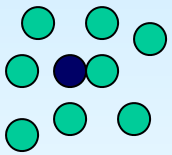


**Recommendation:** Analyze the susceptibility spectra before any fits!

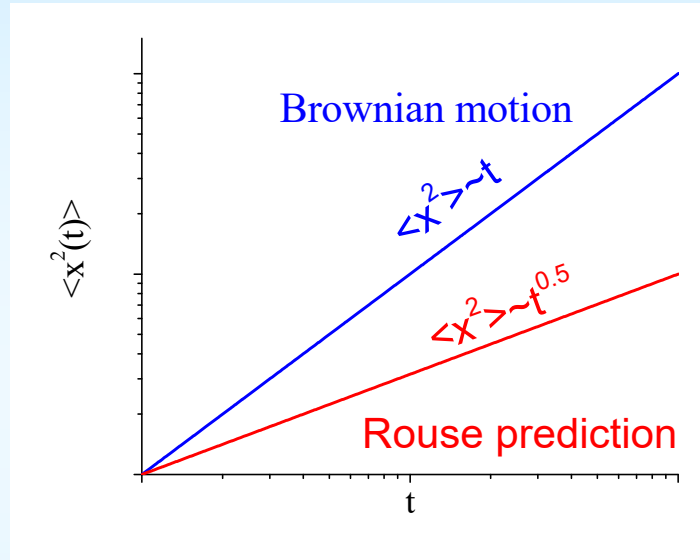
# Chain Dynamics in Polymer Melts

Wisla 2015

## System of small molecules

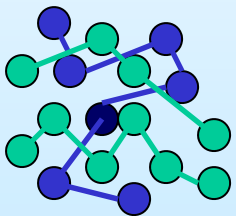


Brownian motion  $\xi \frac{dx(t)}{dt} = f(t)$   $\xi$  is a friction,  $f(t)$  is a random force.



## Polymeric system

Additional force appears in a polymer due to chain connectivity.

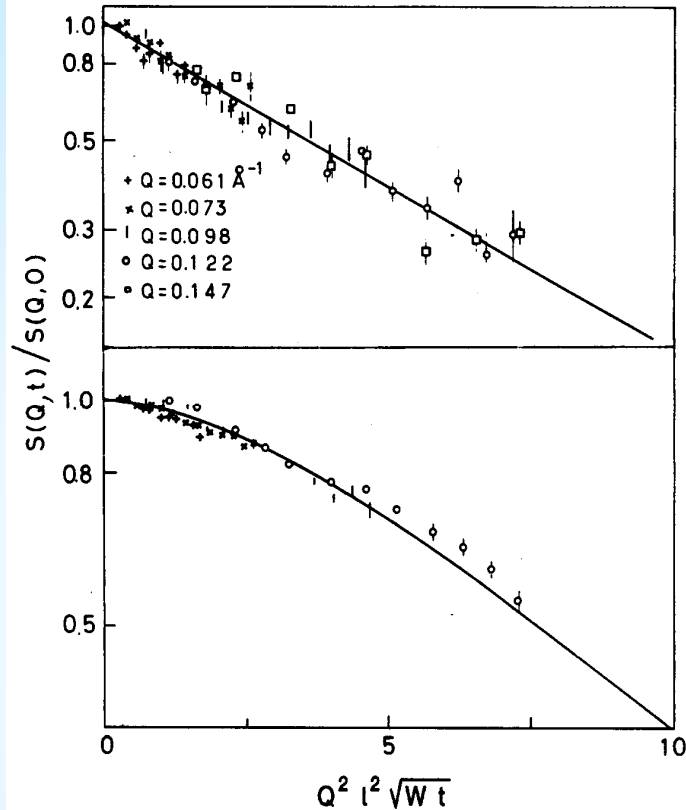


Rouse model assumes Gaussian statistics of the chain and:

It predicts:  $\langle x^2 \rangle \sim t^{0.5}$

$$\xi \frac{dx(t,n)}{dt} = \frac{3T}{a^2} \frac{\partial^2 x(t,n)}{\partial^2 n} + f(t)$$

# Rouse Modes



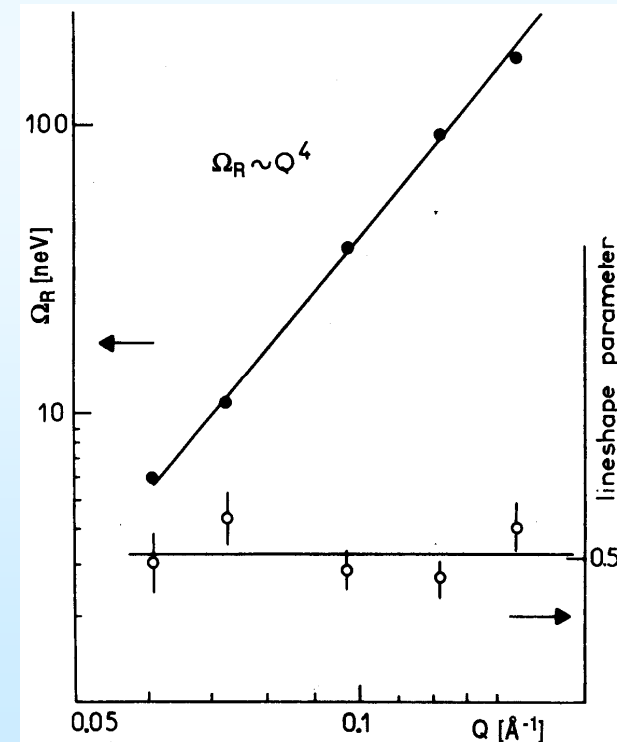
According to the Rouse model,

$$S_{inc}(Q,t) \propto \exp(-Q^2 r^2) \propto \exp(-Q^2 l^2 \sqrt{Wt})$$

Here,  $l$  is a segment length,  $W$  is a friction term.

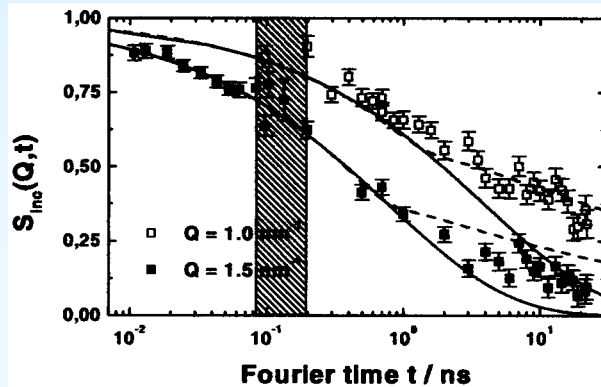
Neutron spin-echo results on partially deuterated PDMS [Ewen, Richter, *Adv.Polym.Sci.* 134, 1 (1997)] show good scaling with the Rouse variable  $Q^2 t^{1/2}$ . No adjustable parameters have been used to scale data measured at different  $Q$ .

The characteristic decay rate  $\Omega = \tau^{-1}$  varies  $\propto Q^4$ , and the stretching parameter  $\beta \sim 0.5$ , in agreement with the predictions of the Rouse model.



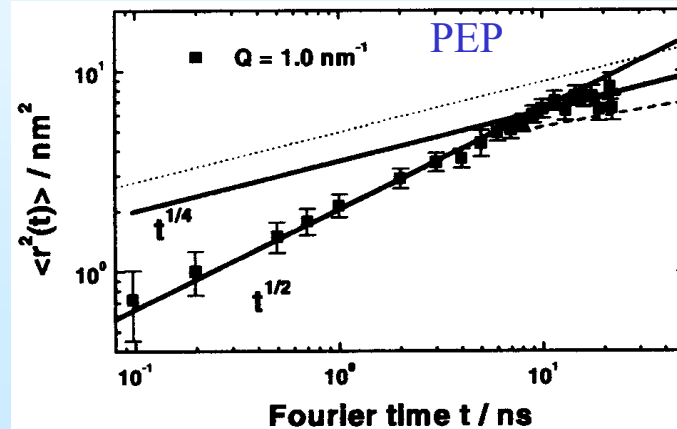
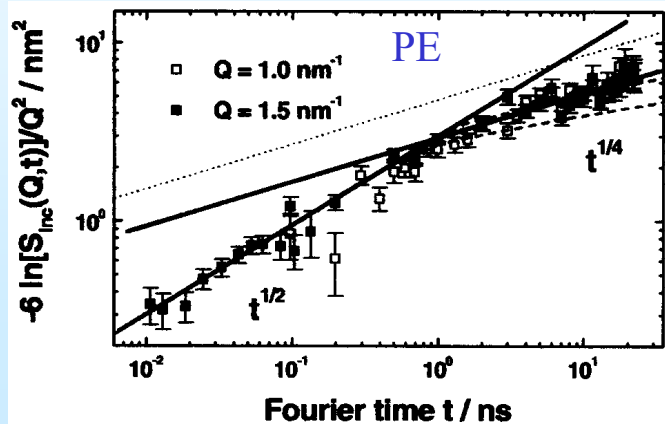
# Entangled Polymers: Reptation regime

When polymer chains are long, their motion is additionally restricted by entanglements with other chains. Reptation model describes a segment diffusion as a motion in a tube with a diameter  $d$  of the order of the distance between entanglements. It predicts  $\langle r^2 \rangle \propto t^{1/2}$  (Rouse regime) at short time scale and distance and much slower  $\langle r^2 \rangle \propto t^{1/4}$  at  $r > d$ .



Intermediate scattering function first decays according to the Rouse regime (the solid lines), but then decay becomes slower [Wischniewski, et al. PRL 90, 058302 (2003)].

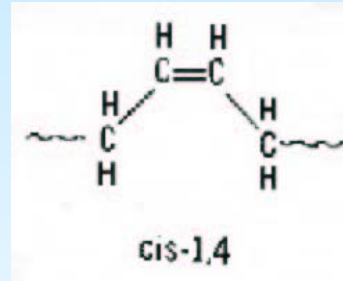
Mean-squared displacement follows the predicted behavior. The inflection point gives microscopic estimate of the tube diameter  $d$ . It differs from viscoelastic estimates [Wischniewski, et al. PRL 90, 058302 (2003)].



# Coherent Scattering

Wisla 2015

## Polybutadiene

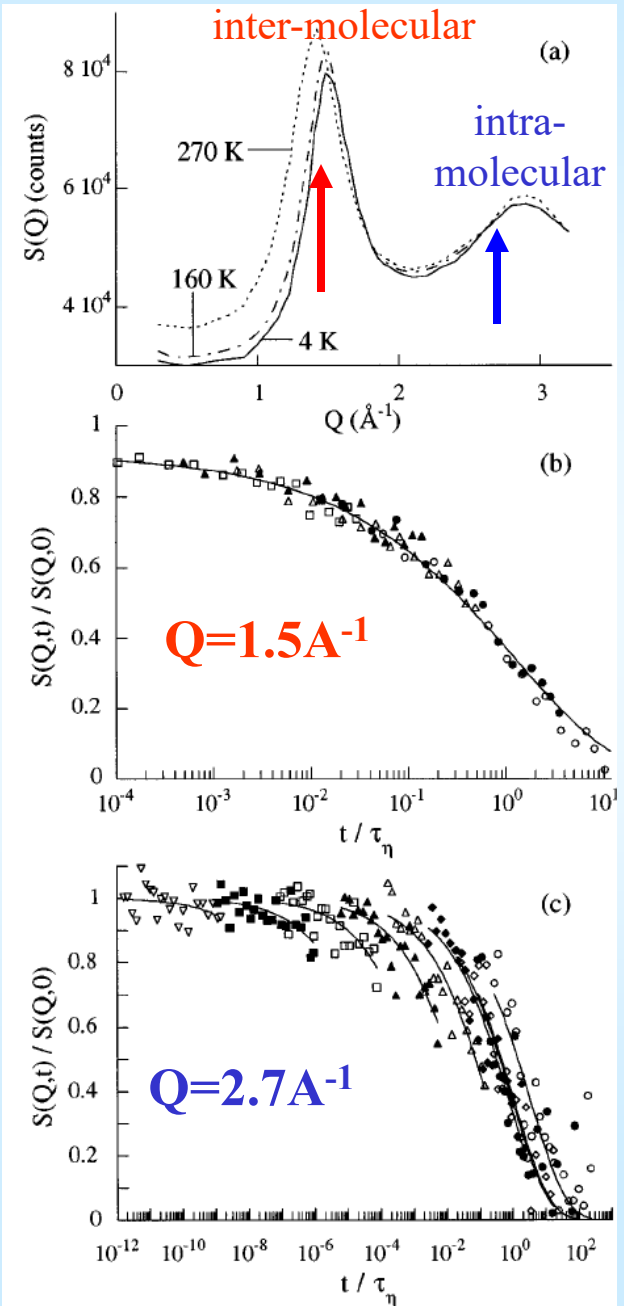


NSE data measured at different  $T$  for deuterated PB scaled with the viscosity time scale  $\tau_\eta$ :

- Master curve for the data measured at  $Q \sim 1.5 \text{ \AA}^{-1}$ ;
- No master curve for the data at  $Q \sim 2.7 \text{ \AA}^{-1}$ .

### Conclusions:

- ✓ Segmental relaxation involves inter-molecular motions;
- ✓ Secondary relaxation involves intra-molecular motion, rotation about the double-bond.



## Advantages of the light scattering are:

- Needs relatively inexpensive experimental setup;
- broad frequency range, three techniques cover total  $10^{-3} - 10^{14}$  Hz;
- good statistics combined with high frequency resolution;
- small probing spot  $\sim 1-10 \mu\text{m}$  allows measurements of very small volumes or of high lateral resolution;
- polarization of light provides additional information on type of motion;
- in most cases the spectra do not require corrections.

## Disadvantages of the light scattering:

- does not measure atomic motion directly, measures fluctuation of  $\epsilon(\mathbf{r},t)$ ;
- wavelength of light,  $\lambda \sim 300-1000 \text{ nm}$ , is much larger than characteristic interatomic distances;
- in many cases requires samples with good optical quality;
- very sensitive to impurities.

## Light Scattering Intensity

Wisla 2015

Light scatters on local fluctuations of dielectric constant  $\delta\epsilon_{yz}(r,t)$ , indexes  $yz$  mean polarizations. The quantities measured in light scattering spectroscopy are either the autocorrelation function of the electric field  $C(t) = \langle E_s(t)E_s^*(0) \rangle$ , or its Fourier transform, the spectrum  $I(\omega)$ .

The electric field of the scattered wave observed at large distance  $R$ :

$$E_s(q, R, t) = \frac{-k_s^2 E_0}{4\pi R \epsilon_0} \delta\epsilon_{yz}(q, t) \exp[i(k_s R - \omega t)]$$

Then intensity is proportional:

$$I(q, \omega) \propto k_s^4 I_0 \int \exp(-i\omega t) dt \langle \delta\epsilon(q, t) \delta\epsilon(-q, 0) \rangle;$$

here  $I_0$  is an incident intensity. Due to small variations of  $|k_s|$  the term  $k_s^4$  is usually neglected in many approximations.

One of the traditional approaches considers  $\delta\epsilon(r,t)$  as a continuous function of  $r$  without going to details of molecular polarizability.  $\delta\epsilon_{yz}(r,t)$ , is expressed in terms of elasto-optic coefficients  $a$  and local deformation tensor  $\gamma_{yz}(r,t)$ :

$$\delta\epsilon_{yz}(r,t) = \underbrace{a_1 \gamma_{iso}(r,t) \delta_{yz}}_{\text{polarized}} + \underbrace{a_2 \tilde{\gamma}_{yz}(r,t)}_{\text{depolarized}}$$

here  $\gamma_{iso}(r,t)$  is an isotropic part of the tensor and  $\tilde{\gamma}_{yz}(r,t) = \gamma_{yz}(r,t) - \delta_{yz} \gamma_{iso}(r,t)/3$  is off-diagonal elements. Thus we have contribution due to longitudinal compression and due to shear deformations. For isotropic fluctuations:

$$g_{iso}(q,t) \equiv a_1^2 \langle \gamma_{iso}(q,t) \gamma_{iso}(-q,0) \rangle \propto \left( \frac{\delta\epsilon}{\delta\rho} \right)^2 \langle \delta\rho(q,t) \delta\rho(-q,0) \rangle = \left( \frac{\delta\epsilon}{\delta\rho} \right)^2 S(q,t)$$

Thus one can measure the same intermediate scattering function like in neutron scattering.

Another approach is based on molecular polarizability picture.  $\delta\epsilon_{yz}(r,t)$  is expressed in terms of an optical polarizability tensor  $\alpha_{yz}(i,t)$ .  $i$  – is an index of the molecule,

$$I_{yz}(q, \omega) = \frac{1}{2\pi} \int_{-\infty}^{\infty} \exp(-i\omega t) dt \left\langle \sum_{i,j} \alpha_{yz}(i,t) \alpha_{yz}(j,0) \exp[iq\{r_i(t) - r_j(0)\}] \right\rangle$$

The correlation function in  $\langle \rangle$  can be decomposed on “self” ( $i=j$ ) and “distinct” ( $i \neq j$ ) correlation functions.

Once again the expression is similar to the neutron scattering  $S(q,\omega)$ . In particular, for polarized scattering,  $y=z$ , of spherical molecules, assuming  $\alpha_{zz}(i,t) = \alpha$

$$I_{zz}(q, \omega) = \frac{\alpha^2}{2\pi} \int_{-\infty}^{\infty} \exp(-i\omega t) dt \left\langle \sum_{i,j} \exp[iq\{r_i(t) - r_j(0)\}] \right\rangle = \alpha^2 S(q, \omega)$$

However, optical polarizability of the molecule depends on surrounding, density, etc. Thus the analysis is not so straightforward as in the case of neutron scattering.

## Advantages:

- scatter on charge density, i.e. nearly directly on atoms;
- wavelength is comparable with interatomic distances;
- good statistics.

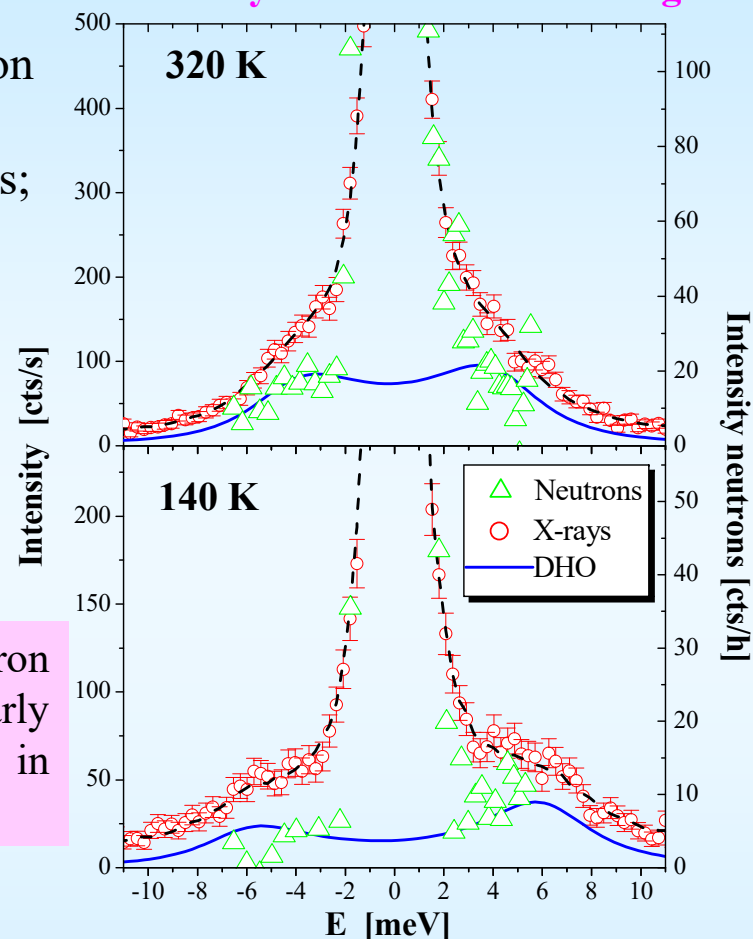
## Disadvantages:

- bad frequency resolution, at present  $\sim 300$  GHz;
- high energy of photons, leads to samples degradation;
- Only a few spectrometers are available in the world

A comparison of inelastic X-ray and neutron scattering [Sokolov, et al. *PRE* 60, R2464(1999)] clearly demonstrates much higher ( $\sim 10^5$ ) count rate in the case of X-ray.

**X-Ray Photon Correlation Spectroscopy (X-PCS)** is analogous to usual PCS. It could be very important technique, but high energy of photons destroys samples too fast.

## Brillouin X-ray and neutron scattering in PB



The absolute intensities were scaled at the first maximum  $Q=1.5\text{\AA}^{-1}$ .

The comparison demonstrates a reasonable agreement.

- Scattering techniques, although significantly more complicated and time-demanding than dielectric spectroscopy, provide additional important information – *geometry of the motion*.
- *Neutron scattering is currently the best technique* to analyze microscopic details of molecular and atomic motions. *X-ray scattering* becomes more efficient and competitive. It provides analysis of slower dynamics if the sample is radiation stable.
- *Light scattering* is also very efficient method for analysis of dynamics. However, the wavelength of light is too large to probe molecular scale details. It is efficient for large-scale motions.
- Combining accurate dielectric measurements with scattering techniques provide one of the most efficient experimental ways to study microscopic mechanisms of molecular motions.